

Euclidean solutions of Yang-Mills-dilaton theory

Yves Brihaye ^{*}

*Dep de Mathématiques et Physique Théorique,
Université de Mons, Place du Parc, 7900 Mons, Belgique*

George Lavrelashvili [†]

*Department of Theoretical Physics,
A.Razmadze Mathematical Institute,
GE-0193 Tbilisi, Georgia
(Dated: February 2, 2008)*

Abstract

Classical solutions of the Yang-Mills-dilaton theory in Euclidean space-time are investigated. Our analytical and numerical results imply existence of infinite number of branches of dyonic type solutions labelled by the number of nodes of gauge field amplitude W . We find that the branches of solutions exist in finite region of parameter space and discuss this issue in detail in different dilaton field normalization.

PACS numbers: 11.27.+d, 11.15Kc, 04.20.Jb

^{*} Brihaye@umh.ac.be

[†] lavrela@itp.unibe.ch

I. INTRODUCTION

Bartnik and McKinnon (BK) discovery of static, spherically symmetric, globally regular solutions of the Einstein-Yang-Mills (EYM) theory [1] has opened new avenue of research in General Relativity. Soon after BK discovery related (colored) black holes were found and different generalisations were investigated (see e.g. [2] for review and references). Interesting modification of pure EYM theory is inclusion of a dilaton field, which is predicted from many modern theoretical considerations like string theory and extra dimensions. So, EYM-dilaton theory was investigated [3, 4, 5] and solitons and black holes similar to BK case were found. It came as a surprise that even eventually simpler YM-dilaton system in flat space-time has infinite tower of globally regular solutions [6, 7, 8] similar to the BK case. These solutions can be labelled by an integer n - number of nodes of gauge field amplitude. The lowest solutions in EYM and (E)YM-dilaton theory have one node and the whole tower of solutions turns out to be unstable with n^{th} solution having $2n$ unstable modes: n in ‘gravitational’ sector and n in ‘sphaleron’ sector [9, 10, 11, 12].

Note that most of these investigations were performed in four dimensional space-time with Lorentzian signature. In such case it was found that electric part of non-abelian $SU(2)$ gauge field should necessarily vanish for asymptotically flat solutions [13, 14]. Situation is changed in Euclidean sector: electric field here plays role similar to the Higgs field in Lorentzian sector. Euclidean version of the EYMD theory was investigated [15] and solutions with non-vanishing electric field and non-vanishing non-Abelian charges were found recently.

The aim of present paper is to study Euclidean solutions in the YM-dilaton theory. The rest of the paper is organized as follows: in next Section we formulate our model, derive equations of motion and asymptotic behaviour of finite action solutions. In Sect. III we discuss some special solutions of our system. In Sect. IV we present our numerical results. Sect. V contains concluding remarks.

II. THE MODEL

Starting point of our investigation is the Euclidean version of Yang-Mills theory coupled to a dilaton field ϕ :

$$S_E = \int \left(\frac{1}{2} \partial_\mu \phi \partial^\mu \phi + \frac{e^{2\gamma\phi}}{4g^2} F_{\mu\nu} F^{\mu\nu} \right) d^4x , \quad (1)$$

where $F_{\mu\nu}$ is the non-Abelian gauge field strength and γ and g denote the dilatonic and gauge coupling constants, respectively.

A. The Ansatz and equations

In this study we will restrict ourselves with the $SU(2)$ gauge group and will be interested in spherically symmetric solutions. Following Witten [16, 17] the general spherically symmetric $SU(2)$ Yang-Mills field can be parameterized as follows:

$$A_0^a = \frac{x^a}{r} u(r) , \quad A_j^a = \epsilon_{jak} x_k \frac{1 - W(r)}{r^2} + \left[\delta_{ja} - \frac{x_j x_a}{r^2} \right] \frac{A_1}{r} + \frac{x_j x_a}{r^2} A_2 , \quad (2)$$

with $r = \sqrt{x_i^2}$ being the radial coordinate, $i, j = 1, 2, 3$ are spatial indices and $a, b = 1, 2, 3$ group indices.

The reduced action S_{red} is defined as follows:

$$S_E = \int_0^{\tau_{\max}} d\tau S_{red} , \quad (3)$$

with $\tau = x_0$ being Euclidean time. Without loss of generality we can put $A_1 = A_2 = 0$. The reduced action then reads:

$$S_{red} = \int dr \left(\frac{1}{2} r^2 \phi'^2 + \frac{e^{2\gamma\phi}}{g^2} (W'^2 + \frac{(1-W^2)^2}{2r^2} + \frac{1}{2} r^2 u'^2 + W^2 u^2) \right) , \quad (4)$$

where the prime denotes the derivative with respect to r .

The equations of motion which follow from the reduced action (4) read:

$$W'' = -2\gamma\phi'W' - \frac{(1-W^2)W}{r^2} + Wu^2 , \quad (5)$$

$$u'' = -2\frac{u'}{r} - 2\gamma\phi'u' + \frac{2}{r^2}W^2u , \quad (6)$$

$$\phi'' = -\frac{2}{r}\phi' + \frac{2\gamma e^{2\gamma\phi}}{g^2r^2}(W'^2 + \frac{(1-W^2)^2}{2r^2} + \frac{r^2u'^2}{2} + W^2u^2) . \quad (7)$$

The rescaling

$$\phi \rightarrow \frac{\phi}{\gamma} , \quad r \rightarrow \frac{\gamma}{g}r , \quad u \rightarrow \frac{g}{\gamma}u , \quad (8)$$

removes the gauge and dilatonic coupling constants g and γ , respectively, from the equations of motion. We thus set without loosing generality $\gamma = g = 1$ in the following.

B. Asymptotic behaviour

Close to $r = 0$ we find a 3-parameter family of solutions regular at the origin, which can be parameterized in terms of b , u_1 and ϕ_0 :

$$W(r) = 1 - br^2 + O(r^4) , \quad (9)$$

$$u(r) = u_1r - \frac{u_1}{2}r^2 + O(r^3) , \quad (10)$$

$$\phi(r) = \phi_0 + 2e^{2\phi_0} \left(b^2 + \frac{u_1}{4} \right) r^2 + O(r^3) . \quad (11)$$

The behaviour of the solutions at infinity is more involved. Assuming a power law behaviour for u and ϕ , for leading behaviour of W we obtain expressions containing the Whittaker functions, which in leading order decay exponentially. We thus obtain:

$$W(r) = Ce^{-u_\infty r} r^{Q_e} \left(1 + O\left(\frac{1}{r}\right) \right) , \quad (12)$$

$$u(r) = u_\infty - \frac{Q_e}{r} + O\left(\frac{1}{r^2}\right) , \quad (13)$$

$$\phi(r) = \phi_\infty - \frac{Q_d}{r} + O\left(\frac{1}{r^2}\right) . \quad (14)$$

So, at infinity there are five free parameters $\phi_\infty, u_\infty, Q_e, Q_d$ and C .

Note that the shift of dilaton field $\phi \rightarrow \phi + \tilde{\phi}$ for any *finite value* $\tilde{\phi}$ can be compensated by a rescaling of r and u as follows:

$$r \rightarrow r e^{\tilde{\phi}}, \quad u \rightarrow u e^{-\tilde{\phi}}. \quad (15)$$

This symmetry can be used to normalize the solutions e.g. as $\phi(r=0)=0$ or $\phi(r=\infty)=0$, and reduces the number of free parameters in the system by one.

III. SPECIAL SOLUTIONS

A. Analytic solutions

The equations of motion (5), (6), (7) have three important analytic solutions. The first one is the vacuum solution with

$$W(r) = \pm 1, \quad u(r) = 0, \quad \phi(r) = 0. \quad (16)$$

The second one is a simple, dyonic-type generalization of dilatonic monopole solutions which have been found previously in the case for $u(r)=0$ [7]:

$$W(r) = 0, \quad u(r) = \bar{u}, \quad \phi(r) = \ln\left(\frac{r}{1+r}\right), \quad (17)$$

where \bar{u} is an arbitrary constant. As in the pure magnetic case this solution can be obtained by integrating the first order Bogomol'ny-type equation as follows. The reduced action (4) for $W(r)=0$ and $u(r)=\text{const}$ can be written as

$$S_{red} = \frac{1}{2} \int dr \left(r \phi' - \frac{e^\phi}{r} \right)^2 + e^\phi|_0^\infty. \quad (18)$$

Thus for configurations with values $\phi(0)=-\infty$ and $\phi(\infty)=0$ the action (18) has a minimum $S_{red}=1$ and attains this minimum for solutions of the first order Bogomol'ny-type equation

$$r^2 \phi' - e^\phi = 0. \quad (19)$$

Solutions of this equation automatically satisfy the equations of motion (5)-(7) with $W=0$ and $u=\text{const}$. Integrating (19) we obtain the logarithmic behavior (17) for the dilaton field.

The third solution is well known Bogomol'ny-Prasad-Sommerfield (BPS) monopole solution, which in our notations reads:

$$W = \frac{r}{\sinh(r)}, \quad u = \coth(r) - \frac{1}{r}, \quad \phi = 0. \quad (20)$$

B. Solutions for $u=0$

The system of Eqs. (5-7) for $u \equiv 0$ was first analyzed in [6] and it was shown that a series of solutions exist indexed by the number of nodes n (with $n \geq 1$) of the function W . In the

normalisation $\phi(0) = 0$ each of these solutions can be uniquely characterized by a value of the ‘shooting’ parameter b entering in (9); for the first few n we have

$$b_1 \approx 0.26083 , \quad b_2 \approx 0.35352 , \quad b_3 \approx 0.37500 . \quad (21)$$

The precise numerical values of parameters b_n for $n = 1, \dots, 8$ can be found in [8]. The solutions with a higher number of nodes are very well approximated on an increasing domain of r by

$$W(r) = \frac{\tilde{W}_1}{\sqrt{r}} \sin \left(\frac{\sqrt{3}}{2} \ln r + \delta \right) , \quad u(r) = 0 , \quad \phi(r) = \ln r , \quad (22)$$

which is solution of the linearized equation of W

$$W'' + \frac{2}{r} W' + \frac{1}{r^2} W = 0 , \quad (23)$$

with \tilde{W}_1 and δ arbitrary constants. The limiting solution with infinitely many zeros of W described by the asymptotic behavior (22) has $b \rightarrow b_\infty \approx 0.37949$.

The values of masses (reduced action) of static solutions in the normalisation $\phi(\infty) = 0$ lie between $M_1 \approx 0.80381$ for the solution with one node and $M_\infty = 1$ for the limiting solution [6, 8].

C. Related Bessel function

In the case of a non-zero electric field, the nature of limiting solution is changed. For

$$u = q \quad \text{and} \quad \phi = \ln r , \quad (24)$$

for the gauge amplitude W in the linear regime, $W \ll 1$, we get equation

$$W'' + \frac{2}{r} W' + \left(\frac{1}{r^2} - q^2 \right) W = 0 , \quad (25)$$

whose solution is a spherical Bessel function

$$W(r) = W_{\text{bessel}} \equiv \frac{\tilde{W}_2}{\sqrt{r}} K_{\frac{i\sqrt{3}}{2}}(qr) , \quad (26)$$

where \tilde{W}_2 is an arbitrary constant.

The function W_{bessel} has the following properties, where for convenience we use $x = qr$. For $x \gg 1$ the solution decays according to $W = \exp(-x)(1/x + O(1/x^2))$. Close to the origin the solution is not analytic. Solving the equation numerically, we see that for $x < 1$ the solution develops oscillations whose amplitudes become larger while the limit $x \rightarrow 0$ is approached. This is illustrated on Fig. 1. The first nodes appear for

$$x_1 \approx 0.0367 , \quad x_2 \approx 0.001 , \quad x_3 \approx 0.000026 . \quad (27)$$

These zeros are separated by extrema, alternatively maxima and minima. The first of these points appear at

$$\tilde{x}_1 \approx 0.1265 , \quad \tilde{x}_2 \approx 0.0032 , \quad \tilde{x}_3 \approx 0.0008 . \quad (28)$$

where, up to an arbitrary normalisation, W takes values

$$W(\tilde{x}_1) = 1 , \quad W(\tilde{x}_2) \approx -6.12 , \quad W(\tilde{x}_3) \approx 35.56 \quad (29)$$

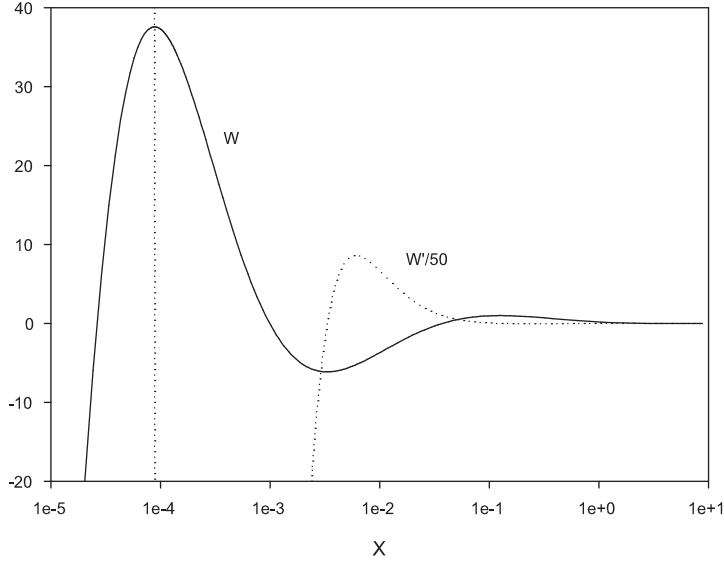


FIG. 1: The solution of the Bessel equation (25). W and W' are plotted as functions of x .

IV. NUMERICAL RESULTS

A. Solutions in the gauge $\phi(\infty) = 0$

We have solved the above equations numerically using the differential equations solver COLSYS [18]. To construct these solutions, we use the following boundary conditions:

$$W(0) = 1, \quad u(0) = 0, \quad \phi(r)'|_{r=0} = 0 \quad (30)$$

at the origin and

$$W(\infty) = 0, \quad u(\infty) = u_\infty, \quad \phi(\infty) = 0 \quad (31)$$

at infinity. The parameters b^{res} , u_1^{res} , u_∞^{res} and mass M^{res} for the solutions in the normalization $\phi_\infty = 0$ are related to the parameters b , u_1 , u_∞ and mass M in the normalisation $\phi_0 = 0$ with a simple shift and rescaling:

$$\phi_0^{res} = -\phi_\infty, \quad b^{res} = e^{2\phi_\infty} b, \quad u_1^{res} = e^{2\phi_\infty} u_1, \quad u_\infty^{res} = e^{\phi_\infty} u_\infty, \quad M^{res} = e^{-\phi_\infty} M. \quad (32)$$

Practically, $u(\infty)$ is the parameter that is fixed by hand in the boundary conditions. From a numerical solution with fixed n and $u(\infty)$ one can extract the values of u_1 and b , and other parameters which enter in asymptotic behaviour Eqs. (9-11) and Eqs. (12-14).

We studied in details the solutions of the above equations with zero, one and two nodes of the gauge field function $W(r)$. Examples of such solutions are given in Fig. 2-4. for $u^{res}(\infty) = 0.1$ respectively for the gauge field function $W(r)$ for zero, one and two nodes, and the corresponding profiles for the functions u and ϕ .

B. Pattern of the solutions

In order to relate the pattern of solutions available for $u \neq 0$ to the solutions of [6],[8] we convert our solutions to the normalization $\phi_0 = 0$ by (32). The values of the two “shooting

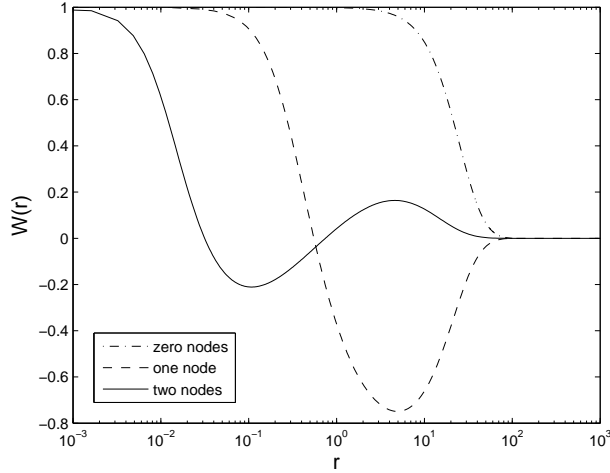


FIG. 2: The gauge field function W is shown for zero, one and two node-solutions, respectively, for $u^{res}(\infty) = 0.1$.

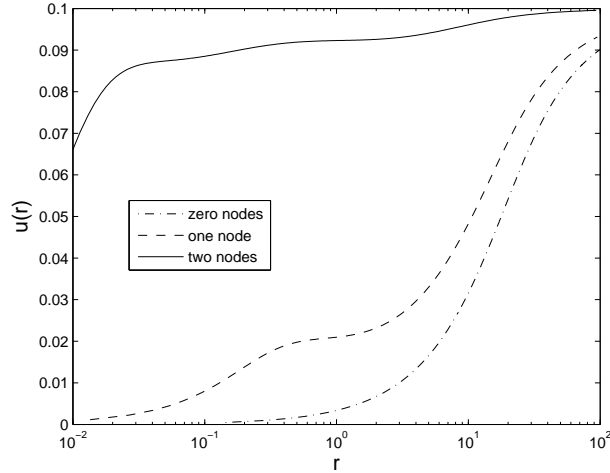


FIG. 3: Same as Fig.2 for the gauge field function u^{res} .

parameters” b and u_1 then fully characterize the solutions and describe a point $P(b, u_1)$ on a plot of initial data. On the $u_1 = 0$ -axis, the numerical values found for b agree with the solutions of [6] and leads to the points $(b_n, 0)$ where b_n are given with a high accuracy in [6],[8].

The relations between parameters b , u_∞ and $u_1 > 0$ are shown in Figs. 5-7. Let us first discuss Fig.5 where the values of b are plotted as functions of the parameter u_∞ for the first few values of n . We see immediately that a branch with no node of the function W exist. In the limit $u_\infty \rightarrow 0$ the function W converge to the constant value $W = 1$ on this branch and we recover vacuum solution Eq. (16). When u_∞ is increasing, b clearly tends to a constant value for $u(\infty) \rightarrow u(\infty)_{cr}$. The actual value of this constant depends on the number of nodes of the gauge field function and increases for increasing number of nodes [19]. Let us point out that when u_∞ becomes large, the solution appears very concentrate in the region

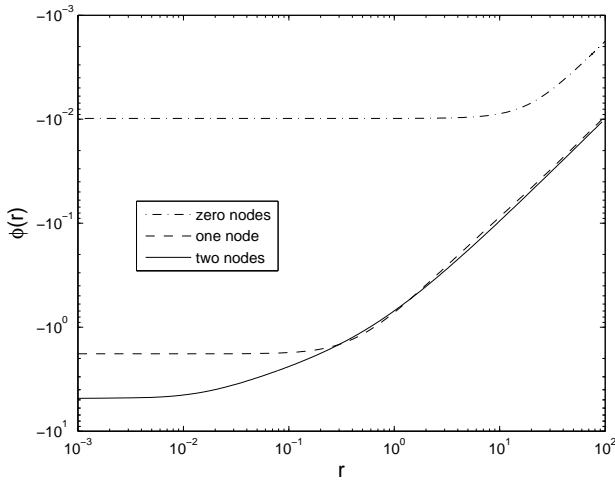


FIG. 4: Same as Fig.2 for the dilaton field function ϕ^{res} .

of the origin and the numerical analysis becomes very difficult.

Complementary to Fig. 5, in Fig. 6 we show the dependence of the parameter u_1 on the parameter $u(\infty)$. The parameter u_1 first increases with $u(\infty)$, reaches a maximal value and then decreases and reaches a constant value for $u(\infty) \rightarrow u(\infty)_{cr}$. Again for a given value of $u(\infty)$, the value of u_1 increases with increasing number of nodes of the gauge field function. Finally, in Fig. 7 we summarize the pattern of the "initial data" of our solutions by presenting the dependence of the parameter b on u_1 . The three curves finish at

$$\begin{aligned} (b, u_1) &\approx (0.3687, 0.2763) & \text{for } n = 0 , \\ (b, u_1) &\approx (0.3796, 0.00707) & \text{for } n = 1 , \\ (b, u_1) &\approx (0.3776, 0.00056) & \text{for } n = 2 . \end{aligned} \quad (33)$$

On this figure we also see in particular the following properties: (i) For $0 < b < b_1$ there exist only solutions with no nodes of W having "monopole asymptotics", $W|_{r \rightarrow \infty} = 0$. An example of such a solution is given by $(b, u_1) = (0.2, 0.2693)$. (ii) For values of b , $b_1 \leq b < b_2$ there exist solutions with zero and one node. Fixing for example $b = 0.27$, they are characterized by the two points $(b, u_1) = (0.27, 0.30222)$ and $(b, u_1) = (0.27, 0.00237)$ and correspond to solutions with monopole asymptotics having zero nodes of W and one node of W respectively. (iii) For values of b such that $b_2 \leq b < b_3$ there exist solutions with zero, one and two nodes. Taking e.g. $b = 0.36$, the three points $(b, u_1) = (0.36, 0.28366)$, $(b, u_1) = (0.36, 0.015866)$ and $(b, u_1) = (0.36, 0.000247)$ with the same parameter b define solutions with monopole asymptotics having respectively zero, one and two nodes of W .

In order to illustrate the critical phenomenon which appears in the large u_∞ limit we refer to Fig.8 and Fig. 9 where the profiles of the one-node solutions are presented for three values of u_∞ . Several properties of the solutions can be observed on these figure. Namely for increasing u_∞ we observe that : (i) the function $u(r)$ increases more and more strongly in the region of the origin and reaches its asymptotic value when W is still very close to $W = 1$; (ii) the dilaton function becomes very close to $\phi(x) = \ln(r)$ in an increasing interval of r where $W(r) \ll 1$. The figures further suggests that the function $W(x)$ approaches closer and closer the profile of the Bessel function between the second extremum and infinity.

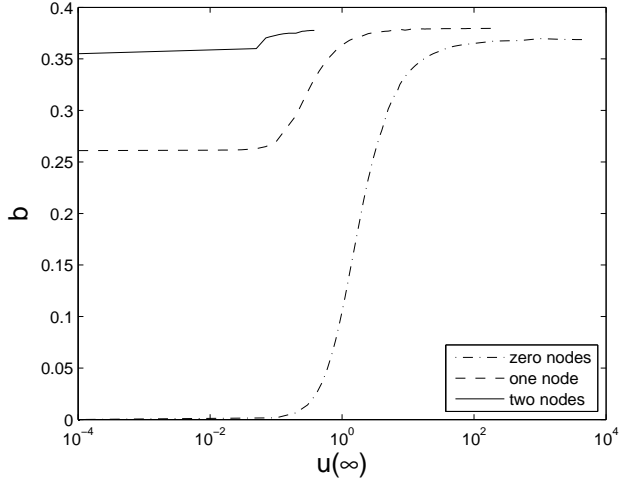


FIG. 5: The dependence of the parameter b on $u(\infty)$ is shown for zero, one and two node solutions.

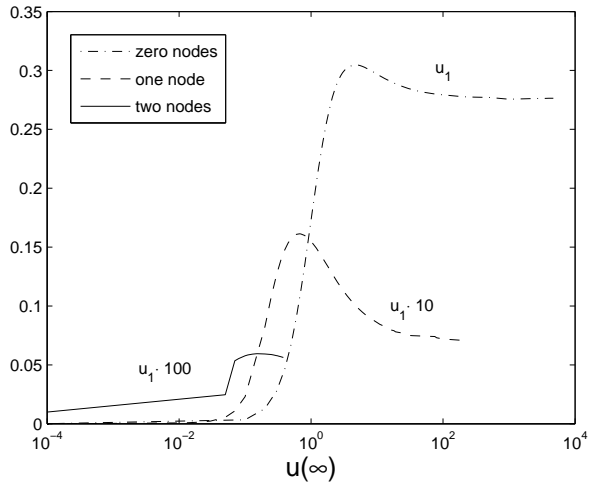


FIG. 6: Same as Fig.5 for the parameter u_1 .

The evidence of this statement is made particularly apparent on Fig.8 where solutions are superposed for three different values of u_∞ and where the corresponding function W_{bessel} is represented by the bullets line. We see in particular that the profiles of W (represented for $u_\infty = 0.5, 1, 10$ respectively by the dotted, dashed and solid lines) become closer and closer to the bullets curve representing the Bessel function (the curve on Fig. 1 has of course to be appropriately renormalized and the argument x has to be rescaled). This rather good fit between the function $W(r)$ presenting n-nodes and the function W_{bessel} breaks down in the region of the origin (the function $W_{\text{bessel}}(x)$ indeed becomes very singular for $x \rightarrow 0$).

To compute the reduced action of the solutions, it is convenient to return to $\phi(\infty) = 0$ gauge. For small values of u_∞ the following behaviour of the reduced action $A \equiv S_{\text{red}}$ is found

$$A \approx 8.9u_\infty \text{ for } n = 0, \quad A \approx 0.803 + 0.5u_\infty \text{ for } n = 1, \quad A \approx 0.965 + 0.1u_\infty \text{ for } n = 2. \quad (34)$$

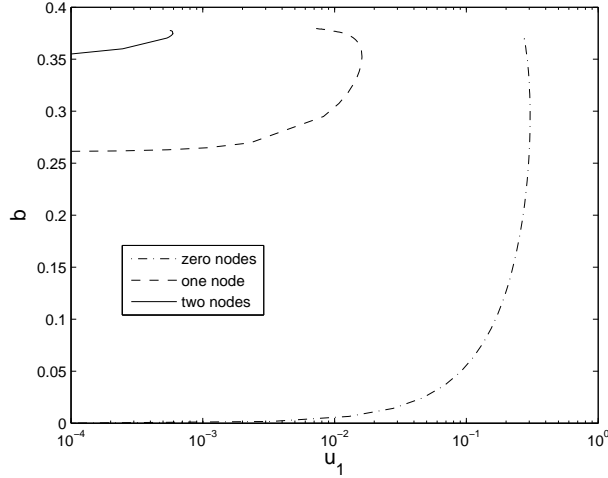


FIG. 7: The plot of initial data is given for the zero, one and two node solutions.

More details of the evaluation of the action for zero-node solutions are shown on Fig. 10. Within our numerical accuracy, we find that $A \rightarrow 1$ in the critical limit as its expected from the property of limiting solution Eq. (17).

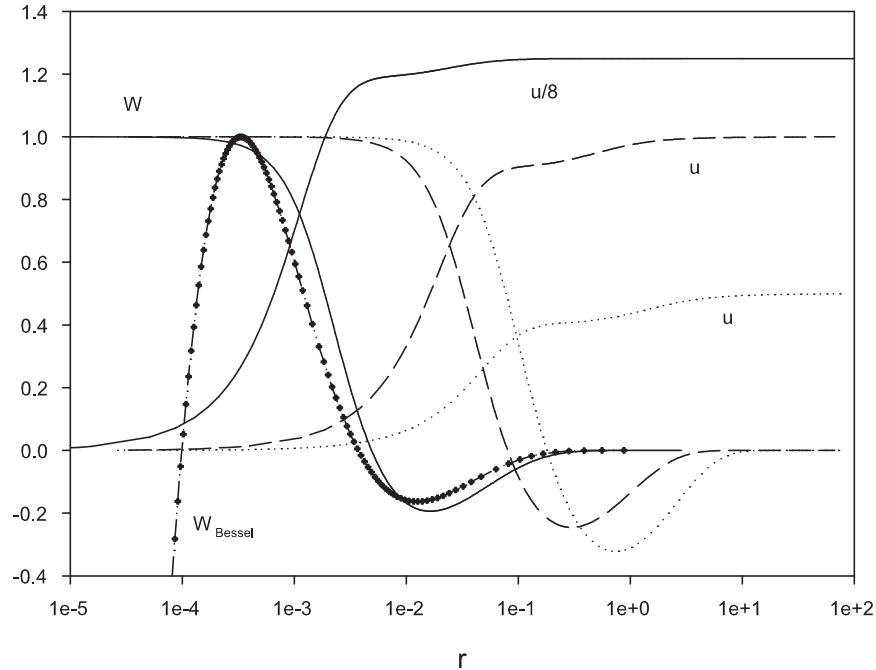


FIG. 8: The profiles of the gauge function W and u for one node solutions are presented for $u_\infty = 0.5, 1.0, 10.0$ respectively by the dotted, dashed and solid lines. The Bessel function is represented by the bullets.

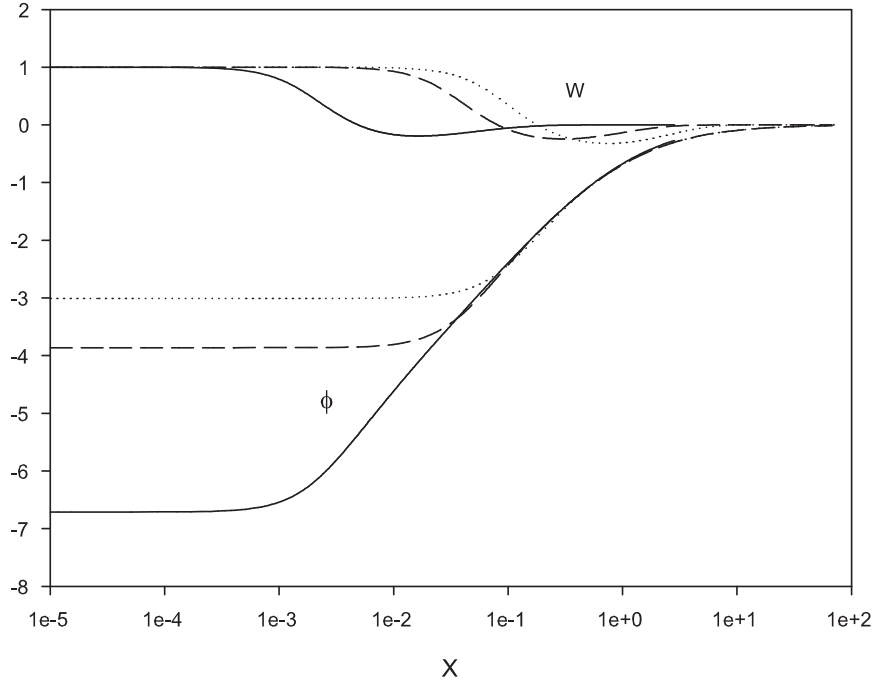


FIG. 9: The profiles of the gauge function W and the dilaton ϕ for one node solutions are presented for $u_\infty = 0.5, 1.0, 10.0$ respectively by the dotted, dashed and solid lines.

C. Solutions in the gauge $u(\infty) = C$

When the equations are analyzed in the ‘gauge’ such that $\phi(\infty) = 0$ and increasing the parameter u_∞ by hand, the solutions become rapidly very concentrated in a region around the origin and the numerics becomes hard, as mentioned already above. As an alternative to understand the critical phenomenon limiting the solutions for a maximal (but n -depending) value of $u(\infty)$, we studied solution with fixed u_∞ and increasing by hand the value $\phi(0)$ as a boundary condition. The value $\phi(\infty)$ can then be determined numerically. Different values for u_∞ can be connected by means of

$$u \rightarrow \Lambda u \quad , \quad r \rightarrow \frac{r}{\Lambda} \quad , \quad \phi \rightarrow \phi - \log(\Lambda) . \quad (35)$$

We will discuss in details the results in this gauge for the solutions with zero and one nodes of W . We would like to point out that no new solutions were discover in the present approach, it is rather a complimentary way of describing the solutions obtained with the normalisation $\phi(\infty) = 0$.

Zero node for W .

Let us first discuss the solution corresponding to zero node of the function W . If we solve the equations with a fixed value for u_∞ and changing the value of $\phi(0)$ by hand, the numerical results show that when $\phi(0)$ decreases, the values $\phi(0)$ and $\phi(\infty)$ become very close to each other and that the function $\phi(x)$ becomes practically constant. As a consequence the equations for $W(r)$ and $u(r)$ reduce to the equations of the monopole of SU(2) gauge theory in the BPS limit. This correspond to the first part of zero node branch labelled ‘1’ on Fig.10.

The fact that the parameter b and u_1 tends to zero in the limit $\phi(0) \rightarrow -\infty$ in the same limit on Figs. 5-7 is due to the fact that the natural radial variable of the monopole solution is rescaled by a factor $\exp(-\phi(0))$, so that the monopole solution appears 'diluted' by the dilaton in the corresponding limit. For small enough $\phi(0)$ this is confirmed by the numerical results which show clearly that the profiles of W , u hardly differ from the (suitably rescaled) BPS solution Eq. (20).

When we increase the value $\phi(0)$, it appears that solutions can be constructed up to a maximal value of this parameter (e.g. we find $\phi(0)_m \approx 0.92$ for $u_\infty = 0.2$) and that a second part of this branch of solutions exists, terminating at $\phi(0) = \phi(0)_m$. It is labelled '2' on Fig.10. When we decrease $\phi(0)$ on this part of the curve, we observe that the parameter b and the difference $\Delta \equiv \phi(\infty) - \phi(0)$ increases while value of parameter u_1 decreases. However, the numerical results strongly indicate that Δ become very large (likely infinite) for $\phi(0) \sim 0.54$ while b and u_1 stay finite. The numerical analysis become very difficult in this limit. This suggests, however the occurrence of a critical value $\phi(0)_c$ limiting the domain of existence of the second part of this branch in the parameter $\phi(0)$. For this choice of $\phi(0)$, the gap Δ becomes arbitrarily large and the dilaton function is very well approximated by $\phi(r) = \ln(r)$ in the intermediate region.

One node for W

The case of solutions with one node of the function W is also instructive and, we guess, leads to a pattern of solutions corresponding to several nodes of W . Increasing $\phi(0)$ from $\phi(0) = -\infty$, we construct the first part of this branch of solutions corresponding to the deformation (by the field $u(x)$) of the first solution of the sequence of dilaton-Yang-Mills solutions constructed in [6]. This branch of one-node solutions can be constructed up to a maximal value of $\phi(0)$. For instance we find $\phi(0)_m \approx -2.05$ where we have $u_\infty \approx 0.126$, $b \approx 0.318$, $\Delta \approx 2.5$, as shown on Fig.11. This branch is labelled '1' on the figure. When $\phi(0)$ decreases on this part of the curve (which is equivalent to the limit $u_\infty \rightarrow 0$), we observe that the minimum of W (denoted by W_m on the figure) progressively approaches -1 and the solution approaches the solution of [6] with $W(0) = 1$, $W(\infty) = -1$.

However, this is not the end of the story; indeed the second part of this branch of solutions can be constructed for $\phi(0) < \phi(0)_m$. This part of the curve is represented by the label '2' on Fig.11. Like the case of the zero-node solution, it seems that this curve is limited by a critical value of $\phi(0)$. Decreasing $\phi(0)$ on this part of one node branch (which is equivalent to increase u_∞ in reference to Figs. 5-7), we observe that the values of Δ and b increases and value of u_1 decreases and that, again, Δ seems to go to infinity when $\phi(0)$ approaches the critical value $\phi(0)_m$. As a further check of this statement that the Bessel function plays a crucial role in the critical phenomenon, we report on Fig. 11 the numerical value of W_m (the local minimum of $W(r)$) and observe that this quantity approaches the value $W_m \approx -0.16$ on the curve '2'. This coincides with the ratio $W(x_1)/W(x_2)$ given in Eq.(29).

More nodes for W

For solutions with n nodes of W , we expect that the scenario will be similar as the two cases we have analyzed in details. In particular, we conjecture that: (i) the second part of the curve corresponding to $n-$ node branch of solution can be constructed up to a minimal value of the parameter $\phi(0)$; (ii) in the large u_∞ -limit, the gauge function W of the non Abelian Euclidean solutions will approach the profile of the Bessel function between the $n + 1$ -th extremum and infinity; (iii) in this same limit b will approach the absolute value of the second derivative of the function W_{bessel} at the corresponding extremum. Numerical investigation of the two-node solution supports this interpretation. A more involved check of

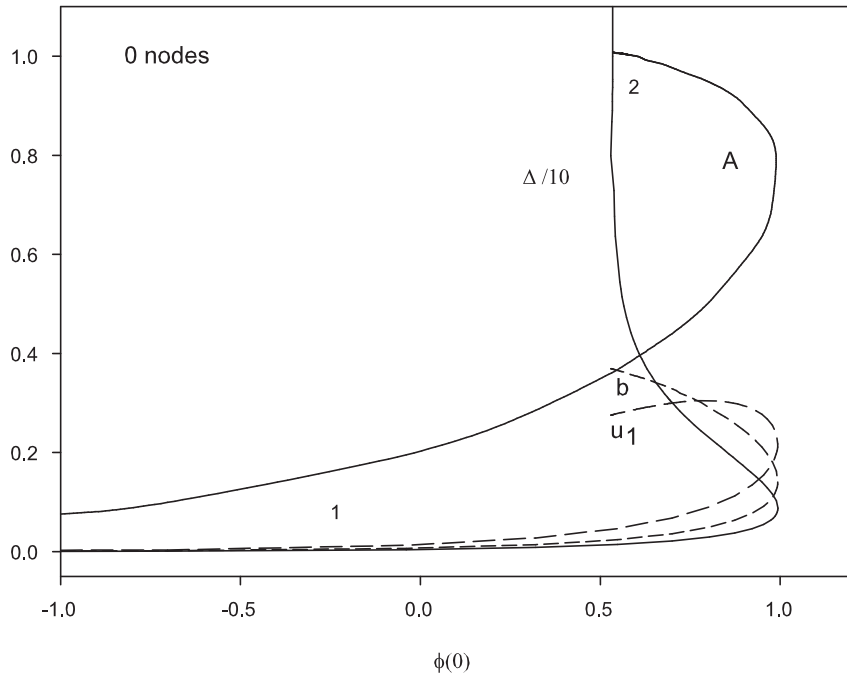


FIG. 10: The parameters $\Delta \equiv \phi(\infty) - \phi(0)$, b and u_1 are plotted as functions of $\phi(0)$ for $u_\infty = 0.2$ for zero node solutions. Curve A represents the values of the corresponding reduced action converted to the gauge $\phi(\infty) = 0$.

this conjecture for generic n would require considerable numerical efforts with our numerical technique or a more refined analytical techniques of the type developed by D. Maison and collaborators [20, 21].

V. CONCLUDING REMARKS

Motivated mainly from string theory we investigated the Euclidean version of a model involving a Yang-Mills field coupled to a dilaton field. We have constructed numerically different branches of finite action solutions of the resulting equations of motion.

Euclidean theory is typically associated to tunnelling processes and to field theory at non-zero temperature. The solutions discussed in the present paper might be relevant to string theory at non-zero temperature. In any case they provide new saddle points in the Euclidean path integral.

Our Euclidean model is very similar to static spherically symmetric sector of spontaneously broken $SU(2)$ gauge theory coupled to a dilaton field, which was investigated in [22, 23] and a discrete family of regular solutions were found corresponding to generalization of the 't Hooft-Polyakov monopoles and their radial excitations. Main difference between Euclidean theory under investigation and static sector of spontaneously broken $SU(2)$ gauge theory is in a way how dilaton field is coupled to electric part of the gauge field resp. Higgs field.

The Yang-Mills-dilaton theory studied in the present paper can be viewed as a limit of

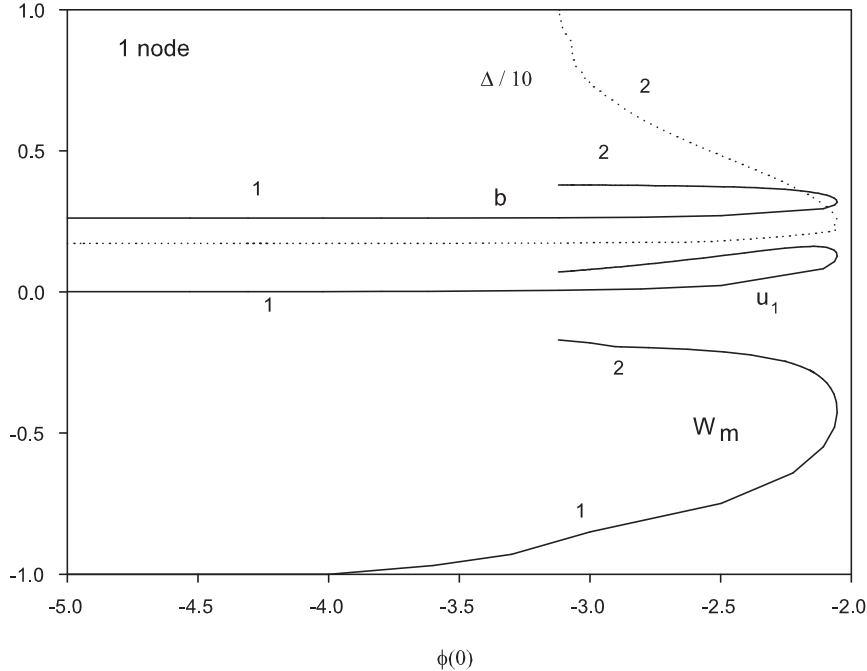


FIG. 11: The parameters $\Delta \equiv \phi(\infty) - \phi(0)$, b , u_1 and the minimal value W_m of the gauge function W are plotted as functions of $\phi(0)$ for $u_\infty = 0.2$ for one node solutions.

vanishing gravitational constant $G \rightarrow 0$ of the Einstein-Yang-Mills-dilaton theory investigated in [15]. Our results might help to find new branches of solutions in Einstein-Yang-Mills-dilaton theory.

An interesting question concerning Euclidean solutions is the number of negative modes in the spectrum of small perturbations about these solutions. It is known that the instanton solutions, which describe mixing between equal energy states have no negative modes (at most have zero modes). Bounce solutions, which describe decay of a metastable vacuum have exactly one negative mode [24, 25, 26, 27]. Whereas presence of more than one negative mode typically shows that there are other solutions with lower action [28]. For better understanding of the role of solutions which we discussed here and for their interpretation it is important to study question of negative modes about them. We plan to come to this topic in further investigation.

Acknowledgements

We are grateful to Dr. Betti Hartmann for numerous discussions at the initial stages of this work and in particular for communicating us some unpublished results on the topic. The main part of G.L.'s work has been done during his visit to Switzerland. He would like to thank the theory group of Geneva University and especially Prof. Ruth Durrer for kind

hospitality and wishes to acknowledge financial support of the Tomalla foundation and SNF.

- [1] R. Bartnik and J. Mckinnon, “Particle - Like Solutions Of The Einstein Yang-Mills Equations,” Phys. Rev. Lett. **61** (1988) 141.
- [2] M. S. Volkov and D. V. Gal’tsov, “Gravitating non-Abelian solitons and black holes with Yang-Mills fields,” Phys. Rept. **319** (1999) 1 [arXiv:hep-th/9810070].
- [3] G. Lavrelashvili and D. Maison, “Regular and black hole solutions of Einstein Yang-Mills Dilaton theory,” Nucl. Phys. B **410** (1993) 407.
- [4] P. Bizon, “Saddle points of stringy action,” Acta Phys. Polon. B **24** (1993) 1209 [arXiv:gr-qc/9304040].
- [5] E. E. Donets and D. V. Galtsov, “Stringy sphalerons and nonAbelian black holes,” Phys. Lett. B **302** (1993) 411 [arXiv:hep-th/9212153].
- [6] G. Lavrelashvili and D. Maison, “Static spherically symmetric solutions of a Yang-Mills field coupled to a dilaton,” Phys. Lett. B **295** (1992) 67.
- [7] P. Bizon, “Saddle point solutions in Yang-Mills dilaton theory,” Phys. Rev. D **47** (1993) 1656 [arXiv:hep-th/9209106].
- [8] D. Maison, “Static, spherically symmetric solutions of Yang-Mills dilaton theory,” Commun. Math. Phys. **258** (2005) 657 [arXiv:gr-qc/0405052].
- [9] N. Straumann and Z. H. Zhou, “Instability Of The Bartnik-Mckinnon Solution Of The Einstein Yang-Mills Equations,” Phys. Lett. B **237** (1990) 353.
- [10] G. V. Lavrelashvili and D. Maison, “A Remark on the instability of the Bartnik-McKinnon solutions,” Phys. Lett. B **343** (1995) 214 [arXiv:hep-th/9409185].
- [11] M. S. Volkov, O. Brodbeck, G. V. Lavrelashvili and N. Straumann, “The Number of sphaleron instabilities of the Bartnik-McKinnon solitons and nonAbelian black holes,” Phys. Lett. B **349** (1995) 438 [arXiv:hep-th/9502045].
- [12] W. H. Aschbacher, “On the instabilities of the static, spherically symmetric $SU(2)$ Einstein-Yang-Mills-dilaton solitons and black holes,” Phys. Rev. D **73** (2006) 024014 [arXiv:gr-qc/0509060].
- [13] A. A. Ershov and D. V. Galtsov, “Nonexistence Of Regular Monopoles And Dyons In The $SU(2)$ Einstein Yang-Mills Theory,” Phys. Lett. A **150** (1990) 159.
- [14] P. Bizon and O. T. Popp, “No hair theorem for spherical monopoles and dyons in $SU(2)$ Einstein Yang-Mills theory,” Class. Quant. Grav. **9** (1992) 193.
- [15] Y. Brihaye and E. Radu, “Euclidean solutions in Einstein-Yang-Mills-dilaton theory,” Phys. Lett. B **636** (2006) 212 [arXiv:gr-qc/0602069].
- [16] E. Witten, “Some Exact Multipseudoparticle Solutions Of Classical Yang-Mills Theory,” Phys. Rev. Lett. **38** (1977) 121.
- [17] P. Forgacs and N. S. Manton, “Space-Time Symmetries In Gauge Theories,” Commun. Math. Phys. **72** (1980) 15.
- [18] U. Ascher, J. Christiansen and R. D. Russell, *A collocation solver for mixed order system of boundary value problems*, Mathematics of Computation **33** (1979), 639; *Collocation software for boundary-value ODEs*, ACM Transactions **7** (1981), 209.
- [19] B. Hartmann, private communication.
- [20] P. Breitenlohner, P. Forgacs and D. Maison, “On Static spherically symmetric solutions of the Einstein Yang-Mills equations,” Commun. Math. Phys. **163** (1994) 141.

- [21] P. Breitenlohner, P. Forgacs and D. Maison, “Classification of static, spherically symmetric solutions of the Einstein-Yang-Mills theory with positive cosmological constant,” *Commun. Math. Phys.* **261** (2006) 569 [arXiv:gr-qc/0412067].
- [22] P. Forgacs and J. Gyurusi, “Static spherically symmetric monopole solutions in the presence of a dilaton field,” *Phys. Lett. B* **366** (1996) 205 [arXiv:hep-th/9508114].
- [23] P. Forgacs and J. Gyurusi, “Magnetic monopole solutions with a massive dilaton,” *Phys. Lett. B* **441** (1998) 275 [arXiv:hep-th/9808010].
- [24] S. R. Coleman, “Quantum Tunneling And Negative Eigenvalues,” *Nucl. Phys. B* **298** (1988) 178.
- [25] A. Khvedelidze, G. Lavrelashvili and T. Tanaka, “On cosmological perturbations in closed FRW model with scalar field and false vacuum decay,” *Phys. Rev. D* **62** (2000) 083501 [arXiv:gr-qc/0001041].
- [26] G. Lavrelashvili, “Negative mode problem in false vacuum decay with gravity,” *Nucl. Phys. Proc. Suppl.* **88** (2000) 75 [arXiv:gr-qc/0004025].
- [27] S. Gratton and N. Turok, “Homogeneous modes of cosmological instantons,” *Phys. Rev. D* **63** (2001) 123514 [arXiv:hep-th/0008235].
- [28] G. Lavrelashvili, “The number of negative modes of the oscillating bounces,” *Phys. Rev. D* **73** (2006) 083513 [arXiv:gr-qc/0602039].